

A facilitative urea transporter is localized in the renal collecting tubule of the dogfish *Triakis scyllia*

Susumu Hyodo^{1,*}, Fumi Katoh², Toyoji Kaneko² and Yoshio Takei¹

¹Laboratory of Physiology and ²Center for International Cooperation, Ocean Research Institute, University of Tokyo, 1-15-1 Minamidai, Nakano, Tokyo 164-8639, Japan

*Author for correspondence (e-mail: hyodo@ori.u-tokyo.ac.jp)

Accepted 20 October 2003

Summary

Reabsorption of filtered urea by the kidney tubule is essential for retaining high levels of urea in body fluids of marine elasmobranchs. To elucidate the mechanisms of urea reabsorption, we examined the distribution of a facilitative urea transporter (UT) in the kidney of the dogfish *Triakis scyllia*. We isolated a cDNA encoding a UT that is homologous to the facilitative UT cloned from another dogfish species, *Squalus acanthias*. The *Triakis* UT mRNA is abundantly expressed in the kidney, while low levels of expression were detected in the brain and liver. In the dogfish kidney, each nephron makes four turns and traverses repeatedly between bundle zone and sinus zone. In the bundle zone, the resulting five tubular segments are arranged in a countercurrent loop fashion. Immunohistochemistry using specific antibodies raised against the cloned UT revealed that, among the nephron segments, the UT is expressed exclusively in the final

segment of the bundle zone, i.e. in the collecting tubule of the *Triakis* kidney. In contrast to the limited localization of UT, the transport enzyme Na⁺/K⁺-ATPase is distributed in the basolateral membrane of numerous tubular segments both in the sinus zone and the bundle zone. However, in the collecting tubule, Na⁺/K⁺-ATPase immunoreactivity was not detected. The present study suggests that the collecting tubule is responsible for the reabsorption of urea in the marine elasmobranch kidney. Other countercurrent segments may contribute to production of a driving force for facilitative diffusion of urea through the UT.

Key words: urea transporter, urea reabsorption, kidney, bundle zone, collecting tubule, Na⁺/K⁺-ATPase, facilitative diffusion, elasmobranch, dogfish, *Triakis scyllia*.

Introduction

To overcome hyperosmotic stress in a marine environment, elasmobranchs maintain their plasma iso-osmotic or slightly hyper-osmotic to surrounding seawater primarily through the retention of urea (see Hazon et al., 1997). Consequently, a large outwardly directed concentration gradient for urea exists between plasma and seawater. Despite this concentration gradient, marine elasmobranchs lose a relatively small amount of urea. An important yet unsolved question is how elasmobranchs maintain the elevated level of urea in their body fluids.

A net influx of water across the body surface caused by the internal hypertonicity of marine elasmobranchs leads to high urine flow rates from the kidney compared with those of marine teleosts. Although urea is freely filtered by the glomerulus, more than 90% of filtered urea is reabsorbed from primary urine by the renal tubules and returned to the blood system, thereby reducing urinary loss of urea (Smith, 1936; Kempton, 1953; Boylan, 1967). Renal excretion thus accounts for only 4–20% of total urea loss (Evans and Kormanik, 1985; Goldstein and Forster, 1971; Payan et al., 1973; Wood et al., 1995). Following transfer from full-strength seawater (SW) to

diluted SW, the plasma urea level is reduced; this reduction is largely attributed to an increase in urea loss at the kidney (see Hazon et al., 1997). These observations imply the existence of a specific mechanism enabling 'uphill' transport of urea by the kidney. Indeed, morphological studies have revealed that the renal tubules of marine elasmobranchs are highly elaborate and show unique features compared with those of other vertebrates (Lacy and Reale, 1985, 1999; Hentschel, 1991; Hentschel et al., 1998). The kidney consists of multiple lobules that are separated into two zones; the bundle zone and the sinus zone (Lacy and Real, 1985), or the lateral bundle zone and the mesial zone (Hentschel et al., 1998). Each nephron makes four turns and traverses repeatedly between the two zones. In the bundle zone, the resulting five tubular segments are arranged to form countercurrent loops. An impermeable peritubular sheath wraps the five tubular segments together and separates tubular bundles from each other.

The bundle of five tubular segments has been considered to play an important role in efficient renal reabsorption of urea in marine elasmobranchs (see Lacy and Reale, 1999). This

hypothesis is supported by the fact that stenohaline freshwater elasmobranchs do not use urea as an osmolyte and lack such countercurrent segments. Nevertheless, a precise mechanism for urea reabsorption has not been clarified yet. This is largely due to difficulty in applying classical physiological methods to the elasmobranch kidney because of its complex architecture. Meanwhile, molecular anatomy can determine the localization of transport proteins for urea, ions and water *in situ*, and thus is a powerful tool to overcome the difficulty in studying the elasmobranch kidney. Spatial patterns in the distribution of various pumps (Hentschel et al., 1993; Swenson et al., 1994), channels and transporters (Biemesderfer et al., 1996) in the nephron segments can provide valuable information on the movement of the above molecules across the kidney tubules, and thus on the reabsorption mechanism of urea.

In the mammalian kidney, facilitative urea transporters (UTs) play a crucial role in the urinary concentration mechanism (see Sands, 2003). Type-A UT proteins (UT-A) are responsible for the high urea permeability of the inner medullary collecting duct and of the thin descending limb of Henle's loop, which participate, respectively, in urea reabsorption and recycling in the kidney. With respect to marine elasmobranchs, Smith and Wright (1999) cloned and characterised a cDNA encoding a UT, which may belong to the mammalian UT-A2 family, from the spiny dogfish (*Squalus acanthias*) kidney. These advances have enabled a more direct approach to the study of the urea reabsorption mechanism by identifying the localization of a UT in the elasmobranch kidney tubules. In the present study, we cloned a cDNA encoding a UT, which is homologous to the *Squalus* UT, from the kidney of the marine dogfish *Triakis scyllia* and determined the localization of the UT in the kidney by immunohistochemistry using specific antibodies raised against the cloned UT. Our study demonstrated that the UT shows a limited localization in the collecting tubule designated by Hentschel et al. (1998), or in the distal segment designated by Lacy and Real (1985). These data suggest that the collecting tubule is responsible for the urea reabsorption in marine elasmobranch kidney.

Materials and methods

Animals

All animal experiments were conducted according to the Guideline for Care and Use of Animals approved by the committee of the University of Tokyo. Japanese banded dogfish, *Triakis scyllia* Muller and Henle, weighing 750–1700 g, were collected in Koajiro Bay, near Misaki Marine Biological Station, University of Tokyo. They were kept without feeding in a 4×10³ litre round tank with running seawater (~12°C) under natural photoperiod for 3–7 days before use. For tissue sampling, fish were anaesthetized in 0.02% (w/v) 3-aminobenzoic acid ethyl ester (Sigma, St Louis, MO, USA).

cDNA cloning of *Triakis* UT

Tissues were dissected out and frozen quickly in liquid nitrogen. Total RNA was extracted from the kidney with

Isogen (Nippon Gene, Toyama, Japan). Poly-A⁺ RNA was purified with Oligotex-dT30 (Japan Synthetic Rubber, Tokyo, Japan). Adaptor-ligated double-stranded kidney cDNA was synthesized using the SMART cDNA Library Construction Kit (Clontech, Palo Alto, CA, USA). A cDNA encoding a portion of UT was amplified from the kidney cDNA with high-fidelity Ex-Taq DNA polymerase (TaKaRa, Kyoto, Japan). The sense and antisense primers were designed based on the amino acid sequences of *Squalus* UT (Smith and Wright, 1999) and mammalian UT-A2 as follows: sense, GTNCARAAAYCCNTGGTGGRC; antisense, CCANGGRTRTRCANCRCRTA. The amplified products were electrophoresed, excised and ligated into pT7Blue T-Vector (Novagen, Madison, WI, USA). The nucleotide sequence was determined by an automated DNA sequencer (PRISM 310; Applied Biosystems, Foster City, CA, USA). Total length of the *Triakis* UT cDNA was obtained by 5'- and 3'-RACE methods with the adaptor primers (Clontech) and the UT gene-specific primers according to the supplier's instructions. Finally, full-length UT cDNA was amplified with newly designed specific primers in the 5'- and 3'-untranslated regions to confirm the sequence.

Detection of UT mRNA expression

The distribution of UT mRNA in *Triakis* tissue was examined by RT-PCR and northern blotting. Poly-A⁺ RNA was isolated from brain, gill, intestine, rectal gland, muscle and liver of three fishes as described above. For RT-PCR, 1 µg of poly-A⁺ RNA was used as template for synthesis of first strand cDNA using Superscript First-Strand Synthesis System for RT-PCR (Invitrogen, Carlsbad, CA, USA). The specific PCR primer pair comprised a sense primer (682–703), CATGGTCTGATCTCAGTGTTC, and an antisense primer (1349–1330), CATCTATGGAAAGAGCAGGG. One fiftieth of RT product was processed for the PCR reaction. After an initial denaturation at 94°C for 1 min, 30 cycles of PCR were performed, each consisting of 50 s denaturation at 94°C, 30 s annealing at 60°C, and 1 min extension at 72°C. Glyceraldehyde-3-phosphate dehydrogenase (GAPDH) mRNA was used as an internal standard. A partial cDNA sequence for *Triakis* GAPDH (deposited to DNA Data Bank of Japan, accession no. AB094994) was obtained by RT-PCR using degenerate primers designed based on other fish GAPDH sequences. RT-PCR for detection of GAPDH mRNA was carried out by the same protocol as for UT, with a sense primer, TCACATTTACAGGGTGGTGC, and an antisense primer, AAGTCAGTTGACACCACCTG. PCR products were electrophoresed in 1.2% agarose gels, stained with ethidium bromide and detected by an FLA-2000 imaging analyzer (Fuji Film, Tokyo, Japan).

For northern blotting, poly-A⁺ RNAs (10 µg or 20 µg) from the kidney, brain, gill and liver were separated in a 1% agarose gel in the presence of 2.2 mol l⁻¹ formaldehyde and transferred to a nylon filter (Nytran-plus; Schleicher and Schuell, Dassel, Germany). The filter was hybridized using a ³²P-labelled UT cDNA probe at 55°C. After washing in 0.1×SSC/0.1% SDS at 55°C, signal was detected by the FLA-2000 imaging analyzer.

Tissue preparation for histochemistry

The kidney was dissected out, trimmed transversely at up to 1 cm thickness and immersed in a fixative solution. The osmolality of fixative containing 4% paraformaldehyde in 0.05 mol l⁻¹ phosphate buffer (pH 7.4) was adjusted to plasma osmolality (1000 mOsm) with NaCl. The tissue was fixed at 4°C for 2 days, washed twice in 70% ethanol at 4°C for 24 h and then embedded in paraplast. Serial transverse sections were cut at 5 µm, mounted onto gelatin-coated slides and processed for immunohistochemistry.

Polyclonal antibody production

The polypeptides ESEATQNPFMKKT and TYPEKN-IRIYQEMKRIEQNK, corresponding to the NH₂ (UTN)- and COOH (UTC)-terminal cytoplasmic domains, respectively, of *Triakis* UT were synthesized and coupled *via* cysteine to keyhole limpet haemocyanin. These conjugated peptides were emulsified with complete Freund's adjuvant and injected into New Zealand white rabbits for immunization (Sawady Technology, Tokyo, Japan). The antisera were subjected to affinity purification with the respective synthetic peptides and were used for immunohistochemistry.

Immunohistochemistry

The kidney sections were immunohistochemically stained with the avidin–biotin–peroxidase complex kit (Vector, Burlingame, CA, USA). After rehydration, tissue sections were incubated sequentially with: (1) 2% normal goat serum in phosphate-buffered saline (pH 7.4; PBS-NGS) for 2 h at room temperature, (2) the affinity-purified anti-UTC or anti-UTN diluted 1:10 000 with PBS-NGS for 48 h at 4°C, (3) biotinylated, goat anti-rabbit IgG for 30 min at room temperature, (4) avidin–biotin–peroxidase complex for 45 min at room temperature and (5) 0.05% diaminobenzidine tetrahydrochloride and 0.01% hydrogen peroxide in 50 mmol l⁻¹ Tris buffer (pH 7.2) for 10 min at 20°C. Adjacent sections were stained with an anti-Na⁺/K⁺-ATPase α-subunit antiserum. The anti-Na⁺/K⁺-ATPase antiserum (a gift from Prof. K. Yamauchi, Hokkaido University, Japan) was raised against a synthetic peptide, VTGVEEGRILFDNLKCC, which represents a completely conserved sequence among all vertebrate groups examined (Ura et al., 1996). To confirm the identity of the epitope, a partial cDNA sequence for *Triakis* Na⁺/K⁺-ATPase α-subunit was obtained by RT-PCR (deposited to DDBJ AB094995).

Specificity of immunoreactive signals for UT was confirmed by (1) comparison of the stained tissues between anti-UTC and anti-UTN antibodies and (2) preabsorption of antibodies with the synthetic antigens (5 µg ml⁻¹) for 24 h at 4°C prior to incubation.

Light micrographs were obtained from a series of stained sections using a digital camera (DXM1200; Nikon, Tokyo, Japan). The nomenclature of the nephron segments was largely based on Hentschel et al. (1998). To determine tubular segments in which the UT is expressed, serial sections (500 µm in thickness) stained with anti-UTC antibody were

investigated. As shown in the Results, immunoreactive signals appeared in the transitional area between the sinus zone and the bundle zone, where immunoreactive tubules were directly connected to the collecting duct. Starting from the origin of immunoreactive signals (either the transitional region or the collecting duct), the convoluted courses of stained tubules were traced on the serial sections. Ten separate nephrons were tested.

Thin sections (2 µm) were cut and used for immunohistochemistry to determine the topical location of the UT on the plasma membrane (apical or basolateral). In this experiment, goat anti-rabbit IgG labelled with Alexa Fluor 488 (Molecular Probes, Eugene, OR, USA) was used as a secondary antibody. Sections were observed with a confocal laser scanning microscope (LSM 310; Zeiss, Jena, Germany).

Western blotting

The kidney was homogenized on ice in a buffer consisting of 25 mmol l⁻¹ Tris HCl (pH 7.4), 250 mmol l⁻¹ sucrose and a pellet (for 50 ml) of Complete Protein Inhibitor (Boehringer Mannheim, Ingelheim, Germany). The homogenate was initially centrifuged at 4500 g for 15 min, and the supernatant was subjected to a second centrifugation step at 200 000 g for 1 h. The pellet was resuspended in the same buffer. All the above procedures were performed at 4°C. The protein content of the sample was quantified with a BCA Protein Assay Kit (Pierce, Rockford, IL, USA). The samples (100 µg) were solubilized in a sample-loading buffer [250 mmol l⁻¹ Tris-HCl (pH 6.8), 2% sodium dodecyl sulphate (SDS), 10% β-mercaptoethanol, 30% glycerol and 0.01% Bromophenol Blue] and heated at 70°C for 15 min. They were separated by SDS–polyacrylamide gel electrophoresis (SDS–PAGE) using 7.5% polyacrylamide gels. After electrophoresis, the protein was transferred from the gel to a polyvinylidene difluoride membrane (Atto, Tokyo, Japan).

The membranes were pre-incubated in 50 mmol l⁻¹ Tris-buffered saline (TBS; pH 7.6) containing 0.05% Triton X-100 and 2% skimmed milk at 4°C overnight and incubated with the antibodies diluted at 1:500 with PBS-NGS for 1 h at room temperature. After rinsing in washing buffer (TBS, 0.05% Triton X-100), the membranes were incubated with gold-conjugated anti-rabbit IgG (British Biocell Inc., Cardiff, UK) for 1 h at room temperature and stained with silver enhancing kit (British Biocell Inc.).

Results

Cloning and expression of *Triakis* UT mRNA

The 5'- and 3'-RACE cloning yielded a 2017 bp cDNA. This cDNA has a polyadenylation site at position 2000 and an open reading frame from nucleotides 33 or 66 to 1205 and putatively encodes a 391 or 380 residue protein (deposited to DDBJ: AB094993; Fig. 1). The *Squalus* UT mRNA also has two possible translation initiation sites, although the second Met residue was designated as position 1 by Smith and Wright (1999). In the central extracellular domain, there is a putative

Fig. 1. Primary structure of the urea transporter (UT) isolated from the kidney of *Triakis scyllia*. The deduced amino acid sequence is aligned with those of the *Squalus acanthias* UT (accession number AF257331), rat UT-A2 (U09957) and rat UT-B2 (U81518) using the Clustal algorithm. Amino acid residues identical to the *Triakis* UT are indicated in black. A putative *N*-glycosylation site and polypeptides used as antigens to generate antibodies are indicated with horizontal bars.

N-glycosylation site, which is conserved among all vertebrate UTs (Fig. 1). The *Triakis* protein has quite high homology to *Squalus* UT (87.5%) and also has 59.3% and 55.5% amino acid identity with rat UT-A2 and UT-B2, respectively. The *Triakis* UT does not contain an ALE domain, which is considered a signature sequence for the UT-B. These results show that this protein is a homologue of the *Squalus* UT and probably belongs to the UT-A2 family.

The RT-PCR analysis revealed that the *Triakis* UT is abundantly expressed in the kidney (Fig. 2A). In one fish, low level of signal was observed in the liver. In all fishes, no signal was observed in the brain, gill, intestine or rectal gland. Signal was not detected from the kidney without reverse transcription, demonstrating the absence of genomic DNA contamination. Northern blot analysis of kidney poly-A⁺ RNA also showed an intense band at ~2.3 kb that corresponds well with the cloned cDNA (Fig. 2B). An additional band was observed at ~4 kb, but signal intensity was very low compared with the major band. In accord with the RT-PCR experiment, northern blotting using 20 µg of poly-A⁺ RNA revealed a low level of expression in the liver. A faint band was detectable also in the brain. However, when 10 µg of poly-A⁺ RNA was used for northern analysis, only kidney poly-A⁺ RNA gave a positive signal (data not shown).

Localization of UT in the *Triakis* kidney

As described in other marine elasmobranchs, the *Triakis* kidney consists of multiple, irregular lobules (see Hentschel et al., 1998; Lacy and Reale, 1985). Each lobule is further separated into two zones, a sinus (or mesial) zone and a bundle zone (Figs 3A, 4A). Large renal corpuscles are situated between the two zones (Fig. 4A). The single nephron makes four loops within the lobule. Beginning at a renal corpuscle, the first hairpin and third convoluted loops are situated in the bundle zone, while the nephron forms the second and fourth convoluted loops in the sinus zone (see Fig. 5D). The final tubular segment is connected to the collecting duct. In the bundle zone, the resulting five tubular segments are enclosed

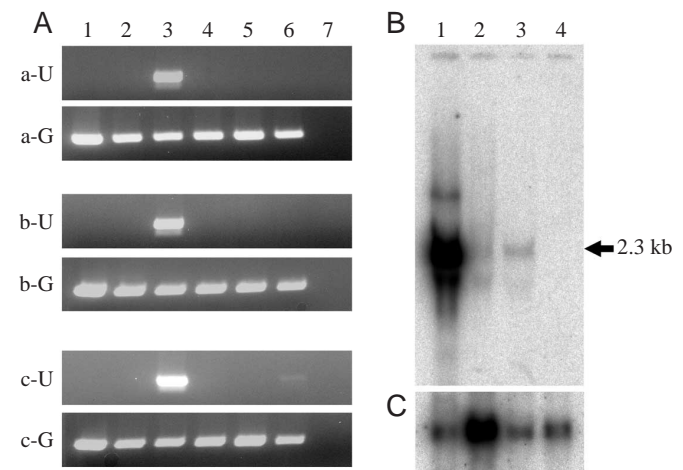
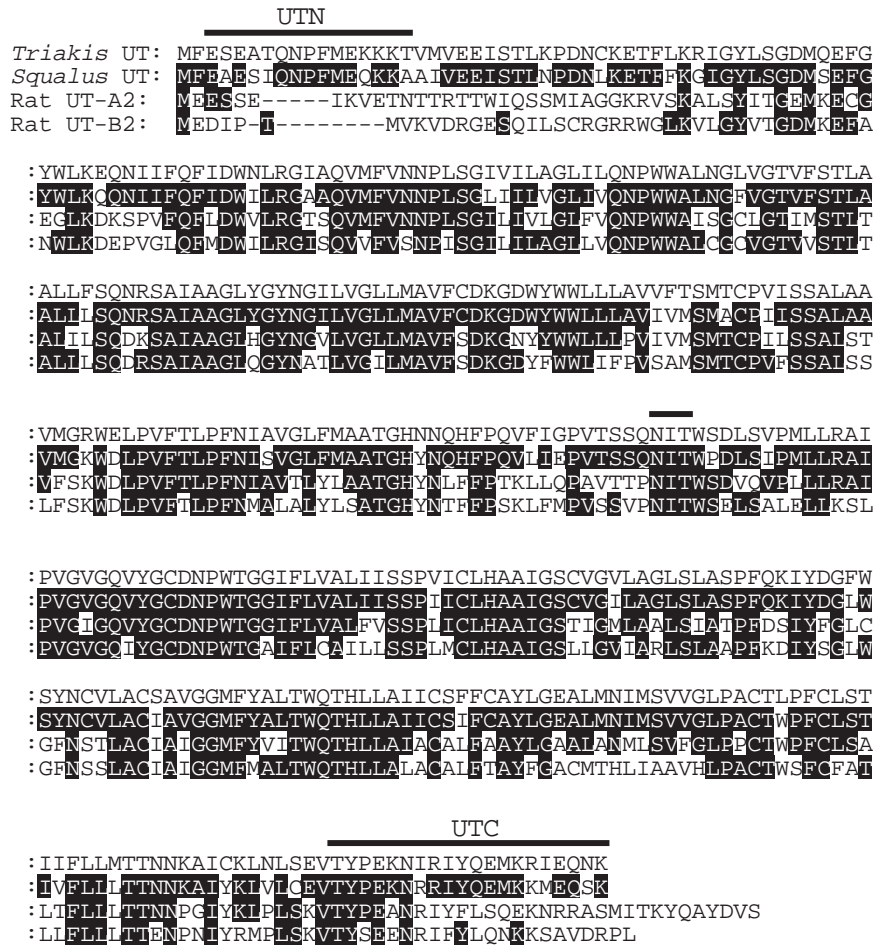


Fig. 2. Expression of the urea transporter (UT) in various tissues of *Triakis scyllia* as examined by (A) RT-PCR and (B,C) northern blotting. (A) PCR was performed using specific primers for *Triakis* UT (U) and *Triakis* GAPDH (G) for three fishes (a-c). Lane 1, brain; 2, gill; 3, kidney; 4, intestine; 5, rectal gland; 6, liver; 7, kidney without reverse transcription. (B,C) 20 µg of poly-A⁺ RNA from the *Triakis* kidney (lane 1), brain (2), liver (3) and gill (4) were electrophoresed and hybridized with the ³²P-labelled UT cDNA (B) and GAPDH cDNA (C) in high stringent condition.

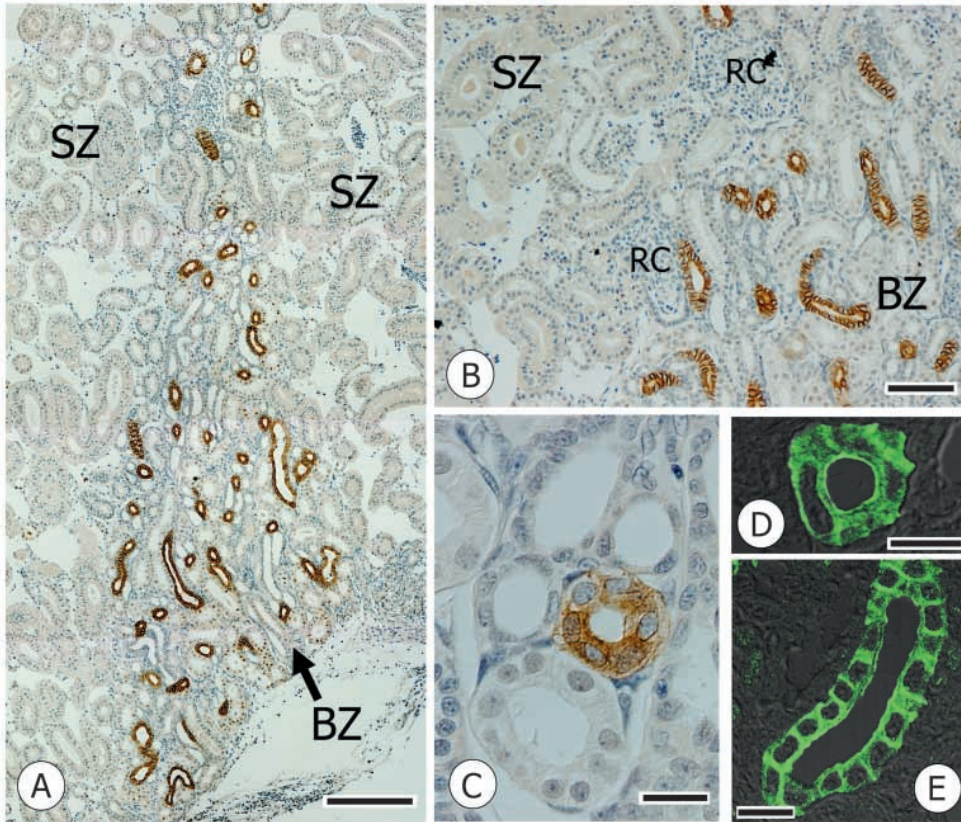


Fig. 3. (A–C) Immunohistochemical localization of the urea transporter (UT; stained in brown colour) in the *Triakis* kidney using antibody raised against the C-terminal peptide of UT. Sections are counterstained with haematoxylin. (A,B) Immunoreactive signal was detected in tubules in the bundle zone (BZ) but not in tubules in the sinus zone (SZ) and in renal corpuscles (RC). (C) Magnified view of five tubular segments in the bundle zone. Only one segment (the collecting tubule) was immunoreactive to UT. (D,E) Confocal laser scanning micrographs of immunoreactive tubules stained with fluorescein-labelled secondary antibody. Cross-sectional view (D) and sagittal view (E) of immunoreactive tubules. Scale bars: A, 200 μm ; B, 100 μm ; C–E, 20 μm .

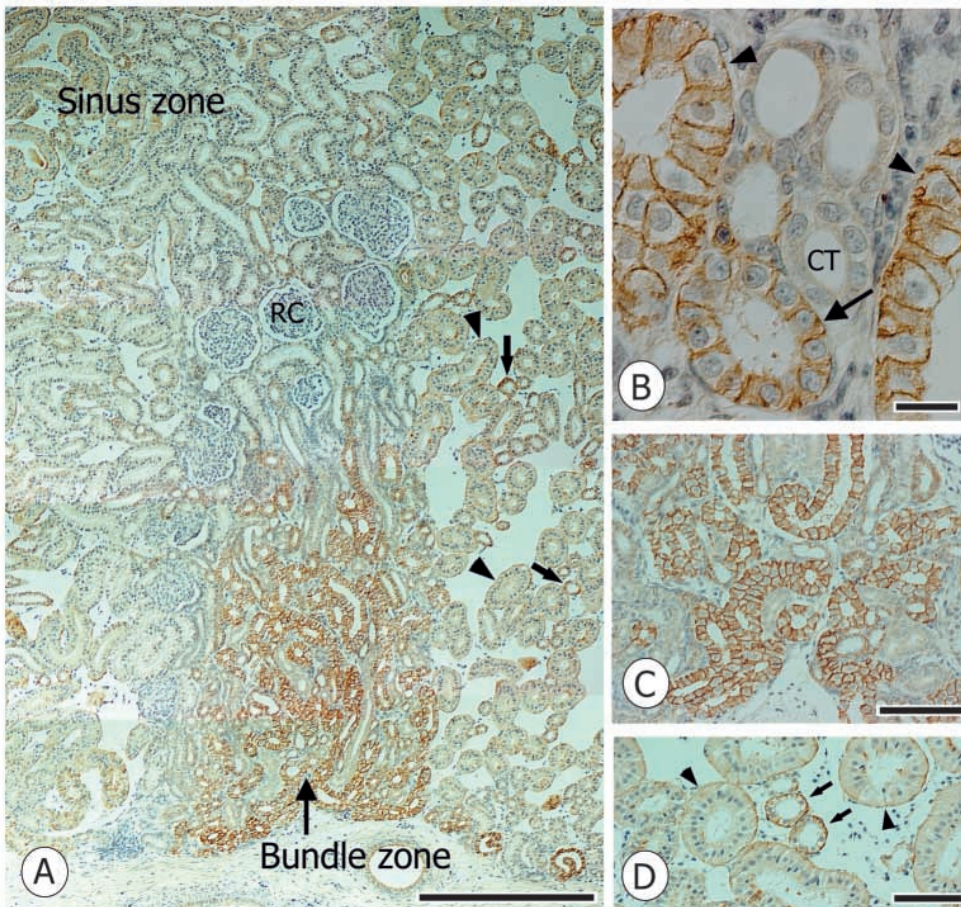


Fig. 4. Immunohistochemical localization of Na^+/K^+ -ATPase (stained in brown colour) in the *Triakis* kidney. Sections are counterstained with haematoxylin. (A) Low power micrograph. Large renal corpuscles (RC) are situated between sinus and bundle zones. The anti- Na^+/K^+ -ATPase antibody stained numerous tubules in both bundle and sinus zones (arrows and arrowheads). (B) Magnified view of five tubular segments in the bundle zone. Intense signal to Na^+/K^+ -ATPase was detected in the ascending limb of the third loop (arrow) and the convoluted early distal segment of the third loop (arrowheads). Na^+/K^+ -ATPase was not detected in the collecting tubule (CT). (C) Magnified view of the convoluted early distal segment at the distal end of the bundle zone. (D) Magnified view of the sinus zone. Intense signal was observed in the basolateral membrane of the intermediate segment (arrows). Arrowheads show the proximal II segment of the second loop. Scale bars: A, 500 μm ; B, 20 μm ; C,D, 100 μm .

in a sac-like peritubular sheath, in which the nephron segments are arranged in parallel to form a countercurrent system.

Immunohistochemistry with the affinity-purified antibody raised against the C-terminal peptide of UT (anti-UTC) revealed positive staining in tubules in the bundle zone but not in tubules in the sinus zone or in renal corpuscles (Fig. 3A,B). In the bundle zone, immunoreactive signal was not detected in every tubule, but only a small proportion of tubules were

stained. Observations on the five tubular segments in the straight portion of bundle zone showed that only one segment was stained with the anti-UTC antibody (Fig. 3C).

The same staining pattern was obtained when an affinity-purified antibody against the N-terminal peptide of UT (anti-UTN) was used as primary antibody (Fig. 6A,B). Treatment with pre-immune sera from the same rabbit revealed no specific signals in the kidney. Preabsorption of the anti-UTC antibody with the synthetic UTC peptide resulted in disappearance of the immunoreactive signals (Fig. 6D), while treatment with the synthetic UTN peptide did not affect immunoreactivity (Fig. 6C). Furthermore, the anti-UTC antibody recognized a single band of molecular mass ~55 kDa by western blot analysis (Fig. 7). This band disappeared when the membrane was incubated with the UTC antibody preabsorbed with the UTC peptide but was not affected by preincubation of the UTC antibody with the UTN peptide (Fig. 7). These results confirmed the specificity of the anti-UTC and anti-UTN antibodies to the *Triakis* UT. Since signal intensity with anti-UTC antibody was much stronger than that with anti-UTN antibody, subsequent analyses were done using only the anti-UTC antibody.

To determine which tubular segments in the bundle zone express the

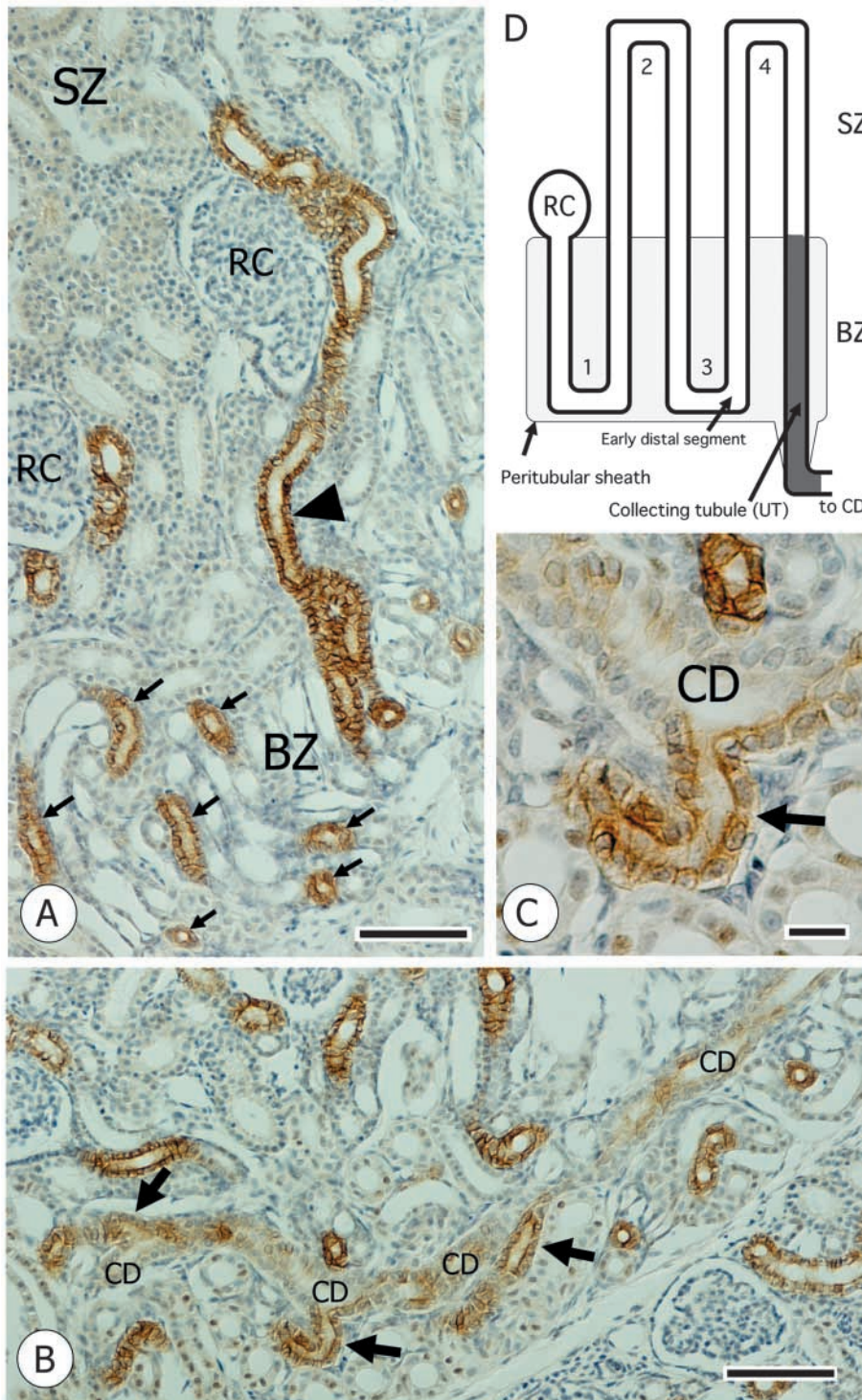


Fig. 5. Identification of the nephron segment immunoreactive to the cloned urea transporter (UT) using antibody raised against the C-terminal peptide of UT. (A) Immunoreactive tubules in the bundle zone representing the straight portion (arrowhead) and the convoluted portion (arrows) of the collecting tubule. (B) Immunoreactive tubules (arrows) are connected directly to the collecting duct (CD) in the bundle zone. (C) Magnified view showing the connection between the immunoreactive tubule (arrow) and the collecting duct (CD). (D) Schematic drawing of the course of a single nephron and of the segment expressing the UT. UT was expressed only in the collecting tubule, the final segment in the bundle zone, in the kidney of *Triakis scyllia*. Each nephron makes four turns (1-4) and traverses repeatedly between the sinus zone (SZ) and the bundle zone (BZ). The resulting five tubular segments in the bundle zone are enclosed in a peritubular sheath. RC, renal corpuscle. Scale bars: A,B, 100 μ m; C, 20 μ m.

UT, serial sections were stained with anti-UTC antibody. Immunoreactive signal appeared in the transitional area between the sinus zone and the bundle zone (Fig. 5A). Immunoreactive tubules were in close association with renal corpuscles and then extended into the bundle zone. The tubules ran straight along with the other tubules to the periphery of the bundle zone (arrowhead in Fig. 5A) and then convoluted (arrows in Fig. 5A). These tubules were finally connected to the collecting duct that ran towards the adjacent bundle (Fig. 5B,C). We traced the convoluted course of the immunoreactive tubules for 10 separate nephrons, as described in the Materials and methods, and confirmed that all immunoreactive tubules in the bundle zone correspond to the collecting tubule, the final nephron segment (Fig. 5D). Other tubular segments, namely the first and third loops in the bundle zone, were negative in UT-staining without exception. Although the signal intensity was not analysed quantitatively, the strongest signal was observed in the straight portion of the collecting tubules. The collecting ducts were also stained; however, the signal intensity was very weak compared with that in the collecting tubules (Fig. 5B,C).

The confocal laser scanning microscopy further revealed that both the apical and basolateral membranes of epithelial cells were positively stained in the collecting tubule (Fig. 3D,E).

Localization of $\text{Na}^+/\text{K}^+-\text{ATPase}$

In contrast to the UT staining pattern, the $\text{Na}^+/\text{K}^+-\text{ATPase}$ antibody stained numerous tubules in both bundle and sinus

zones, indicating that the $\text{Na}^+/\text{K}^+-\text{ATPase}$ is widely distributed along the nephron (Fig. 4). In the sinus zone, at least three nephron segments were easily identified. A large tubule, consisting of extremely tall, columnar-shaped cells (arrowheads in Fig. 4A,D), probably corresponds to the proximal II segment of the 2nd convoluted loop (Hentschel et al., 1998). A thin layer of squamous cells formed the epithelium of the intermediate segment (arrows in Fig. 4A,D), while the third segment of intermediate size is composed of cuboidal cells. The third-type tubule may correspond to the fourth convoluted loop of the nephron, i.e. the late distal segment (see Fig. 5D). The basolateral membrane of most tubular cells in the sinus zone showed $\text{Na}^+/\text{K}^+-\text{ATPase}$ -immunoreactivity to varying degrees. The strongest signal was observed in the basolateral membrane of the second-type, intermediate segment (arrows in Fig. 4A,D).

In the bundle zone, intense immunoreactive signal to $\text{Na}^+/\text{K}^+-\text{ATPase}$ was detected in the largest segment, which consisted of large cuboidal epithelial cells (Fig. 4A–C). $\text{Na}^+/\text{K}^+-\text{ATPase}$ was stained along the basolateral membrane. The distal end of the bundle zone was occupied by this intensely stained segment, suggesting that the $\text{Na}^+/\text{K}^+-\text{ATPase}$ -expressing tubule is the early distal segment of the third loop (Fig. 4C; arrowheads in Fig. 4B; convoluted intermediate segment IV of Lacy and Reale, 1985). This early distal segment extends into the straight portion of the bundle as the ascending limb of the third loop. Indeed, among the five tubular segments of the straight portion of the bundle, only one segment consisting of large cuboidal cells was intensely stained with $\text{Na}^+/\text{K}^+-\text{ATPase}$ (arrow in Fig. 4B), supporting the notion that convoluted and ascending segments of the

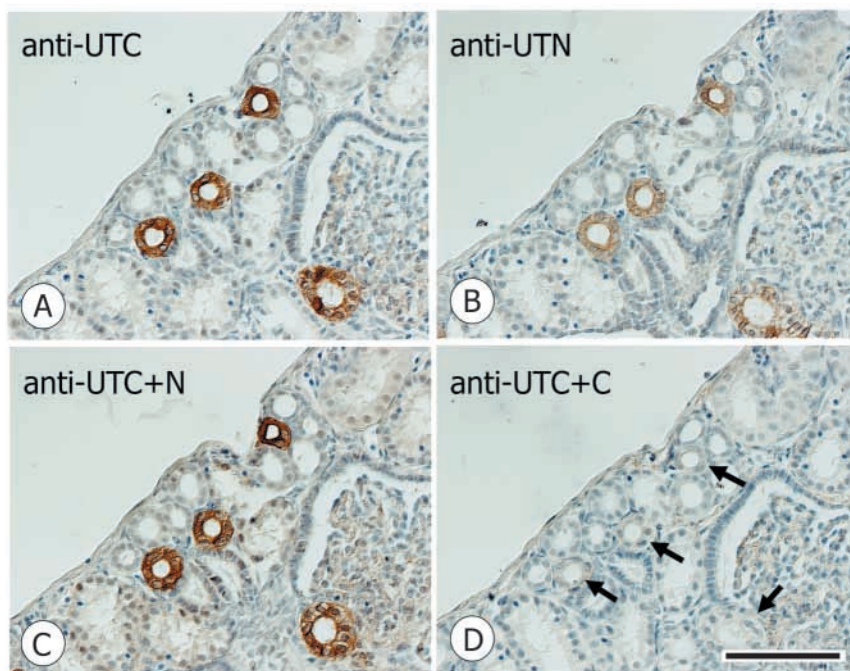


Fig. 6. Specificity check of the urea transporter (UT) antibodies by absorption test. (A,B) The same nephron segments were stained with antibodies raised against the C-terminal peptide (anti-UTC) and N-terminal peptide (anti-UTN) of the UT. Treatment of the anti-UTC antibody with the UTN peptide did not affect immunoreactivity (C), while preabsorption with the UTC peptide resulted in complete extinction of the immunoreactive signals (arrows in D). Scale bar, 200 μm .

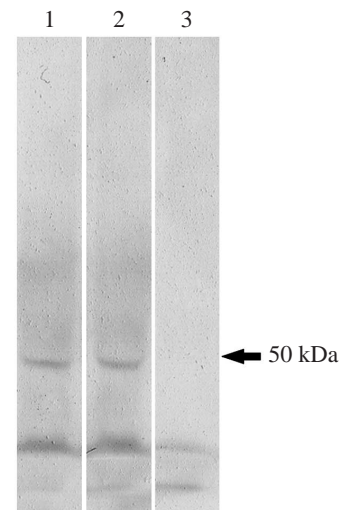


Fig. 7. Western blot analysis using the anti-UTC antibody. The antibody recognized a single band at ~ 55 kDa (lane 1). The signal was not affected by preincubation with the UTN peptide (lane 2), whereas the band disappeared after preabsorption with the UTC peptide (lane 3).

third loop abundantly express Na^+/K^+ -ATPase. The ascending segment stained with Na^+/K^+ -ATPase was frequently in contact with the UT-expressing collecting tubule (Figs 3C, 4B). In the straight portion of the bundle, two other segments, namely the ascending limb of the first loop and the descending limb of the third loop, also express Na^+/K^+ -ATPase, although the intensity was weaker compared with that of the early distal segment (Fig. 4B). The collecting tubule expressing the UT (Fig. 3C) was, without exception, not stained with Na^+/K^+ -ATPase antibody (CT in Fig. 4B).

Discussion

The present study revealed that the UT we have identified is abundantly expressed in the *Triakis* kidney. This tissue-specific expression pattern, together with the sequence similarity, suggests that the *Triakis* UT belongs to the facilitative UT-A family. In the *Triakis* kidney, the UT is localized in the limited nephron segment in the bundle zone. This UT-containing nephron segment is the collecting tubule, because the immunoreactive segment, composed of low cuboidal cells, was connected directly to the collecting duct. These results suggest that the collecting tubule is responsible for the urea reabsorption process in the marine elasmobranch kidney. Because the UT was localized on both apical and basolateral membranes of epithelial cells, urea transport in the collecting tubule could be attributed to passive permeation through the facilitative UT. Other nephron segments in the tubular bundle probably function as a countercurrent multiplier system that produces a driving force for facilitated diffusion of urea. These hypotheses are supported by the previous morphological and physiological studies as shown below, although contribution of other urea-transporting components has also been suggested in the urea reabsorption process.

Boylan and colleagues proposed a model for passive urea reabsorption in the elasmobranch kidney based on anatomical relationships among nephron segments in *S. acanthias* and the little skate *Raja erinacea* (Deetjen et al., 1970; Boylan, 1972). They traced the course of single nephrons following injection of a coloured dye into the glomerulus. The collecting tubule is invested by the first loop in *S. acanthias* and by the first and third loops in the kidney of *R. erinacea*. They proposed that the first and third loops create a low urea interstitial environment by reabsorption of sodium and water. Urea may diffuse from the collecting tubule into the low urea interstitial fluid around it, lowering the urea concentration of the final urine.

Hentschel et al. (1998) examined the vascular system in the bundle zone and its spatial relationship to the surrounding tubular segments in *R. erinacea* and the dogfish *Scyliorhinus caniculus*. They found a single lymph capillary-like central vessel. This capillary system is quite different from the mammalian vasa recta, which functions as a countercurrent exchanging system of blood capillaries in the renal medulla. The central vessel originates as a few blind-ending branches at

the distal end of the bundle and runs in close contact with the collecting tubule, the third loop and, to a lesser degree, the first loop along the entire bundle. In the direction of the sinus zone, the central vessel merges with the large venous sinusoid capillaries of the renal portal system. Based on these observations, they proposed a hypothesis that urea-free fluid is generated in the central vessel by absorbing water and NaCl from the tubules, particularly from a diluting segment. Unidirectional flow of the fluid most likely occurs in the central vessel from the tip of the bundle to the renal portal system because of high resistance at the peritubular sheath and low resistance in the direction of the sinus zone. Countercurrent exchange of urea may then occur from the collecting tubule to the central vessel. Our finding that the *Triakis* UT is specifically localized in the collecting tubule coincides well with these hypothetical models for passive urea reabsorption. Urea may be transported from the filtered urine in the collecting tubule into low-urea interstitial fluid (Boylan, 1972) and/or directly into low-urea fluid in the vascular system (Hentschel et al., 1998) by way of the UT.

Renal micropuncture and microdissection techniques have also been applied to evaluate single nephron functions (Deetjen et al., 1972; Schmidt-Nielsen et al., 1966, 1972; Stolte et al., 1977). In *S. acanthias*, osmotic pressure and urea concentration of fluids obtained from a variety of puncture sites along the proximal tubule were not significantly different from those in plasma, while samples obtained from the ureter had lower osmolality and urea concentration than the blood (Schmidt-Nielsen et al., 1972). Deetjen et al. (1972) did not find any reabsorption of urea in the collecting duct system of *R. erinacea*, indicating that the tubular fluid flowing into the collecting duct has already reached its final low concentration with respect to urea. These physiological data are consistent with our hypothesis that the collecting tubule is responsible for urea reabsorption in the *Triakis* kidney. In our study, immunoreactive UT was also found in the collecting duct, although the signal intensity was quite low compared with the collecting tubule. Thus, the collecting duct may contribute to urea reabsorption to a lesser extent in *T. scyllia*.

In contrast to the preferential localization of UT in the collecting tubule, the transport enzyme Na^+/K^+ -ATPase is widely distributed in tubular epithelial cells in both bundle and sinus zones of the *Triakis* kidney. Among the immunoreactive segments, intense signal was detected in the convoluted and ascending straight portions of the third loop in the bundle zone, corresponding to the early distal segment of Hentschel et al. (1998). This segment seems to be responsible for active NaCl reabsorption. Na^+/K^+ -ATPase immunoreactivity was found in the basolateral membrane of epithelial cells in our study, while immunoreactive $\text{Na}^+/\text{K}^+/\text{2Cl}^-$ cotransporter has been detected along the apical membrane of the early distal segment of *S. acanthias* (Biemesderfer et al., 1996). A microperfusion study has also shown that the early distal segment contains an NaCl reabsorptive activity that is sensitive to furosemide, an inhibitor of $\text{Na}^+/\text{K}^+/\text{2Cl}^-$ cotransporter activity (Friedman and Hebert, 1990). The epithelial cells of the early distal segment

have elaborate basolateral infoldings and numerous large mitochondria that are characteristic of ion-transporting epithelia (Hentschel, 1991). These immunohistochemical and physiological results, together with our present results, suggest that the early distal segment of the elasmobranch kidney is homologous to the thick ascending limb of Henle's loop in the mammalian kidney (Martinez-Maldonado and Cordova, 1990). The early distal segment thus may function as a diluting segment, which contributes to low-urea fluid generation in the interstitium and/or inside the central vessel, since the blind-ending branches of central vessels were closely associated with the early distal segment (Hentschel et al., 1998).

Urea transport in the mammalian nephron is largely due to passive permeation (facilitated diffusion; Hays et al., 1977; Sands, 2003), although recent evidence suggests that an ion-coupled active component may also contribute to this process (Walsh and Smith, 2001; Sands, 2003). To date, at least three components (a sodium/urea cotransporter and antiporters) have been reported in the inner medullary collecting duct of rat kidney (Walsh and Smith, 2001). Thus, the involvement of an unidentified ion-coupled component(s) in the urea reabsorption process cannot be ruled out in elasmobranchs. In fact, in marine elasmobranchs, the presence of a sodium-coupled urea transporter has been suggested in the gill (Fines et al., 2001). Because of its huge surface area exposed to external environments, the gill is another site of urea loss to the environment (Boylan, 1967; Rasmussen, 1971; Haywood, 1977; Evans and Kormanik, 1985; Goldstein and Forster, 1971; Payan et al., 1973). Nevertheless, the urea efflux across the dogfish gill is considerably lower than that across the teleost gill (Part et al., 1998) and across the toad bladder (Payan et al., 1973). This low urea efflux certainly facilitates urea retention in the body. Low permeability to urea in the epithelial cell membrane of dogfish gill is explained by the highest reported cholesterol-to-phospholipid molar ratio (Fines et al., 2001). In addition, analysis of urea uptake revealed the presence of a phloretin-sensitive, sodium-coupled urea antiporter on the basolateral membrane, which returns urea to the blood (Part et al., 1998; Fines et al., 2001). Ouabain, an inhibitor of the Na^+/K^+ -ATPase, suppressed the ATP-dependent urea uptake.

In the kidney, tubular urea reabsorption is tightly coupled with sodium reabsorption at a fixed ratio of 1.6:1 over a wide range of urine flow rates and urea reabsorption values, suggesting the presence of a sodium-coupled urea cotransporter (Schmidt-Nielsen et al., 1972). Walsh and Smith (2001) have pointed out two hypothetical components for active urea transport in the elasmobranch kidney; an apical sodium/urea cotransporter and a basolateral sodium/urea antiporter. In both models, an inwardly directed sodium gradient in the epithelial cell, established by the basolateral Na^+/K^+ -ATPase, provides a driving force for urea movement through the transporters. In the *Triakis* kidney, Na^+/K^+ -ATPase was not detected in the collecting tubule, suggesting that transport (reabsorption) of urea in the collecting tubule occurs transcellularly by facilitated diffusion. The localization

of UT on both apical and basolateral membranes supports this hypothesis. Meanwhile, other nephron segments expressing Na^+/K^+ -ATPase may function as an active component of urea transport.

In conclusion, our molecular anatomical study provides, for the first time, direct evidence showing that the final nephron segment, the collecting tubule, expresses a facilitated UT. Our results suggest that the collecting tubule exerts an important function for urea reabsorption in the *Triakis* kidney. To confirm our hypothesis, physiological evidence for urea permeability through the collecting tubule is necessary. A survey of additional facilitative or sodium-coupled UTs is also required in future studies to delineate the overall mechanism of urea reabsorption in the elasmobranch kidney.

The authors thank Prof. Christopher A. Loretz of State University of New York at Buffalo for critical reading of the manuscript. We are grateful to the Misaki Marine Biological Station, University of Tokyo, for the maintenance of dogfish. We are also indebted to Prof. K. Yamauchi of Hokkaido University for providing anti- Na^+/K^+ -ATPase antibody and to Dr Craig P. Smith of the University of Manchester for informing us of the sequence of *Squalus* UT. This work was supported by Grant-in-Aid for Scientific Research (C) (14540609) to S.H. and (A) (13304063) to Y.T. from the Japan Society for the Promotion of Science and for Creative Basic Research (12NP0201) from the Ministry of Education, Science, Sports and Culture of Japan.

References

- Biemesderfer, D., Payne, J. A., Lytle, C. Y. and Forbush, B., III** (1996). Immunocytochemical studies of the Na-K-Cl cotransporter of shark kidney. *Am. J. Physiol.* **270**, F927-F936.
- Boylan, J. W.** (1967). Gill permeability in *Squalus acanthias*. In *Sharks, Skates and Rays* (ed. P. W. Gilbert, R. F. Mathewson and D. P. Rall), pp. 197-206. Baltimore: Johns Hopkins Press.
- Boylan, J. W.** (1972). A model for passive urea reabsorption in the elasmobranch kidney. *Comp. Biochem. Physiol. A* **42**, 27-30.
- Deetjen, P., Antkowiak, D. and Boylan, J. W.** (1970). The nephron of the skate, *Raja erinacea*. *Bull. Mt. Desert Isl. Biol. Lab.* **10**, 5-7.
- Deetjen, P., Antkowiak, D. and Boylan, J. W.** (1972). Urea reabsorption by the skate nephron: micropuncture of collecting ducts in *Raja erinacea*. *Bull. Mt. Desert Isl. Biol. Lab.* **12**, 28-29.
- Evans, D. H. and Kormanik, G. A.** (1985). Urea efflux from the *Squalus acanthias* pup: the effect of stress. *J. Exp. Biol.* **119**, 375-379.
- Fines, G. A., Ballantyne, J. S. and Wright, P. A.** (2001). Active urea transport and an unusual basolateral membrane composition in the gills of a marine elasmobranch. *Am. J. Physiol.* **280**, R16-R24.
- Friedman, P. A. and Hebert, S. C.** (1990). Diluting segment in kidney of dogfish shark. I. Localization and characterization of chloride absorption. *Am. J. Physiol.* **258**, R398-R408.
- Goldstein, L. and Forster, R. P.** (1971). Osmoregulation and urea metabolism in the little skate *Raja erinacea*. *Am. J. Physiol.* **224**, 367-372.
- Hays, R. M., Levine, S. D., Myers, J. D., Heinemann, H. O., Kaplan, M. A., Franki, N. and Berliner, H.** (1977). Urea transport in the dogfish kidney. *J. Exp. Zool.* **199**, 309-316.
- Haywood, G. P.** (1977). A preliminary investigation into the roles played by the rectal gland and kidneys in the osmoregulation of the striped dogfish *Poroderma africanum*. *J. Exp. Zool.* **193**, 167-176.
- Hazon, N., Tierney, M. L., Anderson, G., Mackenzie, S., Cutler, C. and Cramb, G.** (1997). Ion and water balance in elasmobranch fish. In *Ionic Regulation in Animals* (ed. N. Hazon, F. B. Eddy and G. Flik), pp. 70-86. Berlin: Springer.

- Hentschel, H.** (1991). Developing nephrons in adolescent dogfish, *Scyliorhinus caniculus* (L.), with reference to ultrastructure of early stages, histogenesis of the renal countercurrent system, and nephron segmentation in marine elasmobranchs. *Am. J. Anat.* **190**, 309-333.
- Hentschel, H., Mahler, S., Herter, P. and Elger, M.** (1993). Renal tubule of dogfish, *Scyliorhinus caniculus*: a comprehensive study of structure with emphasis on intramembrane particles and immunoreactivity for H⁺-K⁺-adenosine triphosphatase. *Anat. Rec.* **235**, 511-532.
- Hentschel, H., Storb, U., Teckhaus, L. and Elger, M.** (1998). The central vessel of the renal countercurrent bundles of two marine elasmobranchs – dogfish (*Scyliorhinus caniculus*) and skate (*Raja erinacea*) – as revealed by light and electron microscopy with computer-assisted reconstruction. *Anat. Embryol.* **198**, 73-89.
- Kempton, R.** (1953). Studies on the elasmobranch kidney-II. Reabsorption of urea by smooth dogfish, *Mustelus canis*. *Biol. Bull.* **104**, 45-56.
- Lacy, E. R. and Reale, E.** (1985). The elasmobranch kidney II. Sequence and structure of the nephrons. *Anat. Embryol.* **173**, 163-186.
- Lacy, E. R. and Reale, E.** (1999). Urinary system. In *Sharks, skates, and rays* (ed. W. C. Hamlett), pp. 353-397. Baltimore: Johns Hopkins Press.
- Martinez-Maldonado, M. and Cordova, H. R.** (1990). Cellular and molecular aspects of the renal effects of diuretic agents. *Kidney Int.* **38**, 632-641.
- Part, P., Wright, P. A. and Wood, C. M.** (1998). Urea and water permeability in dogfish (*Squalus acanthias*) gills. *Comp. Biochem. Physiol. A* **119**, 117-123.
- Payan, P., Goldstein, L. and Forster, R. P.** (1973). Gills and kidneys in ureosmotic regulation in euryhaline skates. *Am. J. Physiol.* **224**, 367-372.
- Rasmussen, L. E.** (1971). Organ distribution of exogenous ¹⁴C-urea in elasmobranchs, with special regard to the nervous system. *Comp. Biochem. Physiol. A* **40**, 145-154.
- Sands, J. M.** (2003). Mammalian urea transporters. *Annu. Rev. Physiol.* **65**, 543-566.
- Schmidt-Nielsen, B., Truniger, B. and Rabinowitz, L.** (1972). Sodium-linked urea transport by the renal tubule of the spiny dogfish *Squalus acanthias*. *Comp. Biochem. Physiol. A* **42**, 13-25.
- Schmidt-Nielsen, B., Ullrich, K. J., Rumrich, G. and Long, W. S.** (1966). Micropuncture study of urea movements across the renal tubules of *Squalus acanthias*. *Bull. Mt. Desert Isl. Biol. Lab.* **6**, 35-37.
- Smith, C. P. and Wright, P. A.** (1999). Molecular characterization of an elasmobranch urea transporter. *Am. J. Physiol.* **276**, R622-R626.
- Smith, H. W.** (1936). The retention and physiological role of urea in the elasmobranchii. *Biol. Rev.* **11**, 49-82.
- Stolte, H., Galaske, R. G., Eisenbach, G. M., Lechene, C., Schmidt-Nielsen, B. and Boylan, J. W.** (1977). Renal tubule ion transport and collecting duct function in the elasmobranch little skate, *Raja erinacea*. *J. Exp. Zool.* **199**, 403-410.
- Swenson, E. R., Fine, A. D., Maren, T. H., Reale, E., Lacy, E. R. and Smolka, A. J.** (1994). Physiological and immunocytochemical evidence for a putative H-K-ATPase in elasmobranch renal acid secretion. *Am. J. Physiol.* **267**, F639-F645.
- Ura, K., Soyano, K., Omoto, N., Adachi, S. and Yamauchi, K.** (1996). Localization of Na⁺,K⁺-ATPase in tissues of rabbit and teleosts using an antiserum directed against a partial sequence of the alpha-subunit. *Zool. Sci.* **13**, 219-227.
- Walsh, P. J. and Smith, C. P.** (2001). Urea transport. In *Nitrogen Excretion* (ed. P. A. Wright and P. M. Anderson), pp. 279-307. San Diego: Academic Press.
- Wood, C. M., Part, P. and Wright, P. A.** (1995). Ammonia and urea metabolism in relation to gill function and acid-base balance in a marine elasmobranch, the spiny dogfish (*Squalus acanthias*). *J. Exp. Biol.* **198**, 1545-1558.